

Trinuclear Fragments as Nucleation Centres: New Polyoxoalkoxyvanadates by (Induced) Self-Assembly

Achim Müller,* Jochen Meyer, Hartmut Bögge, Anja Stammler, and Alexandru Botar

Dedicated to Professor Bernt Krebs on the occasion of his 60th birthday

Abstract: The presence of pentaerythritol (C(CH₂OH)₄) in an aqueous vanadate solution leads—depending on the pH value and other specific reaction conditions—to the formation of (CN₃H₆)₄Na₂[H₄V₆^{IV}P₄O₃₀{(CH₂)₃-CCH₂OH}]₂ · 14 H₂O (**1**), Na₆[H₄V₆^{IV}P₄O₃₀{(CH₂)₃CCH₂OH}]₂ · 18 H₂O (**2**), (NH₄)₇[H₇V₁₂^{IV}V₇^VO₅₀(CH₂)₃CCH₂OH] · 11.5 H₂O (**3**), (CN₃H₆)₄[V₃^{IV}V₄^VO₁₉F(CH₂)₃CCH₂OH] · 5.25 H₂O (**4**), Na₆[V₁₀^{IV}V₂^VO₃₀F₂{(CH₂)₃CCH₂OH}]₂ · 22 H₂O (**5**) or (CN₃H₆)₄[V₂^{IV}V₈^VO₂₈F₂-

{(CH₂)₃CCH₂OH}]₂ · 4 H₂O (**6**). The corresponding anions contain as basic structural elements trinuclear {V₃O₁₃} or {V₃O₁₂F} units, which are stabilized by the organic substituent acting as a tripod ligand. It can be assumed in principle that these units act as nucleation centres during the formation

Keywords: clusters · magnetic properties · polyoxometallates · polyoxovanadates · self-assembly

processes of the cluster anions. In this context it is remarkable that the trinuclear units can even occur in a quasi-isolated state, as in the anions of **1** and **4**. The compounds were characterized by IR, UV/Vis/NIR and EPR spectroscopy as well as by magnetochemical investigations and single-crystal X-ray structure determinations. Susceptibility data are especially useful for identifying the trinuclear units as well as the nature of their magnetic coupling with the rest of the structure.

Introduction

The planned synthesis and modification of large transition metal clusters is a challenge of modern inorganic chemistry, particularly when the intention is to obtain materials with tailor-made properties. In the special case of polyoxometallates, the basic principles of organization for synthetic chemistry are gradually becoming better understood.^[1] General problems in this context are the generation in the reaction solution of intermediates which can be linked in various ways. Of special importance is the optimal control of steric and electronic influences which determine not only their formation but also the type of linkage. During the last 20 years the structures of a large number of polyoxometallates have been determined; the overwhelming variety of topologies and electronic structures of the corresponding cluster anions is most unusual in the field of inorganic chemistry.^[2] Among the great variety of different structures, certain frequently occurring fragments can be identified which represent basic

building blocks. An example is the trinuclear {M₃O₁₃} unit, which dominates the chemistry of polyoxotungstates and which is also common to a smaller extent among polyoxomolybdate structures. This unit is built from three {MO₆} octahedra which are joined at the edges and have one common μ₃-O atom (Figure 1). Formally, it can be regarded as

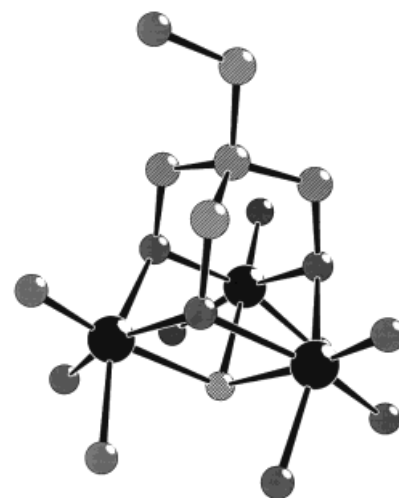


Figure 1. Ball-and-stick model of a trinuclear {V₃^{IV}O₁₃L} (≡{V₃L}) or {V₃^{IV}O₁₂FL} (≡{V₃L}') unit (V: black; O: grey; C: light grey, hatched; μ₃-O or μ₃-F, respectively: white, crosshatched).

[*] Prof. Dr. A. Müller, Dr. J. Meyer, Dr. H. Bögge, A. Stammler, Dr. A. Botar
Fakultät für Chemie der Universität Bielefeld
Lehrstuhl für Anorganische Chemie I
Postfach 100131, D-33501 Bielefeld (Germany)
Fax: (+49) 521 106-6003
E-mail: amueller@cheops.chemie.uni-bielefeld.de

part of one of the well-known Keggin-type ions $[M_{12}O_{36}(PO_4)]^{3-}$ ($M = Mo, W$) in which four $\{M_3O_{13}\}$ units share corners with a central $\{PO_4\}$ tetrahedron. The corresponding structure is not known for $M = V$.

Among the polyoxovanadates, cluster anions containing trinuclear fragments ($\equiv\{V_3\}$) are rare. The main reason for this is the high negative charge density, and therefore high nucleophilicity, of the naked $\{V_3\}$ unit (formally, $\{V_3O_{13}\}^{n-}$; $n = 14$ for V^{IV} , $n = 11$ for V^{V}), which has a correspondingly high affinity for electrophilic groups such as $\{VO\}^{m+}$ ($m = 2, 3$), so that larger condensed cluster aggregates are formed. Examples are species of the type $\{V_{14}O_{38}(EO_4)\}$ ($E = P, V$)^[3] and $\{V_{18}O_{42}(EO_4)\}$ ($E = S, V$)^[4], which can be regarded as enlarged Keggin ions with characteristic $\{VO\}$ caps and which exist with different electron populations.

To prevent this type of growth to higher nuclearity cluster systems, it appears to be possible to trap or stabilize the $\{V_3\}$ fragments, for example by appropriate ligands, which should fulfil two important prerequisites:

- 1) Their geometry has to correlate with the geometry of the $\{V_3\}$ units.
- 2) They should contribute to the decrease in the high charge density.

A possible choice would be trifunctional alcohols of the $(HOCH_2)_3CR$ type (tris(hydroxymethyl)methane derivatives)^[5] which, because of their steric requirements, coordinate without strain with the trinuclear arrangements of the $\{V_3\}$ type (Figure 1) but also reduce the overall charge of the cluster according to the formal Equation (1), where E is a heteroelement such as P. The electronic properties of the ligands can also be varied within certain limits by changing the organic residue R (see ref. [5a]).



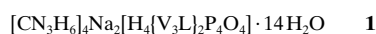
We now report the synthesis and characterization of several polyoxoalkoxyvanadates, some of which have novel types of structure. Their formation apparently involves $\{V_3\}$ units as nucleation centres in the presence of a pentaerythritol ligand ($R = CH_2OH$).

Results and Discussion

The compounds **1–6** were prepared from aqueous vanadate solutions in the presence of pentaerythritol under various reaction conditions (see Experimental Section). They all contain, as a common structural element, trinuclear fragments of the type $\{V_3^{IV}O_{13}(CH_2)_3CCH_2OH\}$ ($\equiv\{V_3L\}$ in **1–3** with $L = (CH_2)_3CCH_2OH$) or, in the presence of F^- , $\{V_3^{IV}O_{12}F(CH_2)_3CCH_2OH\}$ ($\equiv\{V_3L'\}$ in **4, 5**) and $\{V^{IV}V^{V}_2O_{12}F(CH_2)_3CCH_2OH\}$ ($\equiv\{V_3L''\}$ in **6**), respectively, which share corners and edges with other $\{EO_x\}$ polyhedra ($E = V, P$; $x = 4, 5, 6$; see Figure 2). In the $\{V_3L'\}$ and $\{V_3L''\}$ units the μ_3 -O atom of the $\{V_3\}$ unit is substituted by a μ_3 -F atom (Figure 1). As it can be assumed that these units act as nucleation centres which induce or influence the type of aggregation of the $\{EO_x\}$ polyhedra, the term (induced) self-

assembly is justified because a core initially formed in the solution directs the subsequent steps of assembly leading to the final clusters.

Thus the compounds **1–6** are represented by the following abbreviated formulae, where $[CN_3H_6]^+ =$ guanidinium cation and $\{V_3L\}$, $\{V_3L'\}$ and $\{V_3L''\}$ are defined above.



Green crystals of **1** (space group $P\bar{1}$) can be isolated from a solution containing hydrogenphosphate ions at pH 8 (Table 1). The centrosymmetric anion $[H_4\{V_3L\}_2(PO_4)]^{6-}$ (**1a**) consists of two $\{V_3L\}$ units which can be transformed into each other by a (crystallographic) inversion centre and which are linked by four $\{PO_4\}$ tetrahedra (Figures 2, 3). The distances within the trinuclear units are 320 ($V1-V2'$), 321 ($V1-V3$) and 336 pm ($V2'-V3$), respectively. The reason for the significantly greater distance between $V2'$ and $V3$ can be attributed to the fact that the oxygen atom bridging the two metal centres ($O5$) also interacts strongly with a sodium cation of the crystal lattice (see Figure 3). The shortest distance between the vanadium atoms of two different trinuclear units is 462 pm. The oxidation states of the metal centres as well as the positions of the protons are evident from bond valence sum calculations^[6] (Table 2). Permanganometric redox titrations confirm the presence of six V^{IV} centres. Two of the four protons are located at the two μ_3 -O atoms of the two trinuclear units and the other two (disordered) at two of the four terminal oxygen atoms belonging to the phosphate groups. The sodium and guanidinium cations can be determined unambiguously from difference Fourier maps; the sodium atoms coordinate with three bridging oxygen atoms of the two $\{V_3P_2O_5\}$ rings of the cluster anion and complete their octahedral-type ligand sphere by coordinating with three oxygen atoms of the crystal water molecules (Figure 3).

The structure of the anion of **2** is nearly identical to that of **1**, but the replacement of the guanidinium cations leads to a different organization of the crystal packing. The anions of **2** are linked along the crystallographic c axis by four sodium cations, thus forming a chain motif (Figure 4), with the consequence that the cluster anions are more densely packed in the crystal lattice than in **1**. The shortest distance between the inversion centres of neighbouring anions is 1092 pm in **1**, but only 558 pm in **2**.

Compound **3** crystallizes in the acentric space group $P2_12_1$ and can be regarded formally as a derivative of the known mixed-valence isopolyvanadate $(NH_4)_7[H_{10}V_{12}^{IV}V_7^{VO_{50}}] \cdot 12H_2O$ (**7**).^[7] The anions of **3** and **7** are built from a total of seven $\{VO_4\}$ tetrahedra and twelve $\{V^{IV}O_6\}$ octahedra, six of which form two $\{V_3\}$ units located at the poles of the

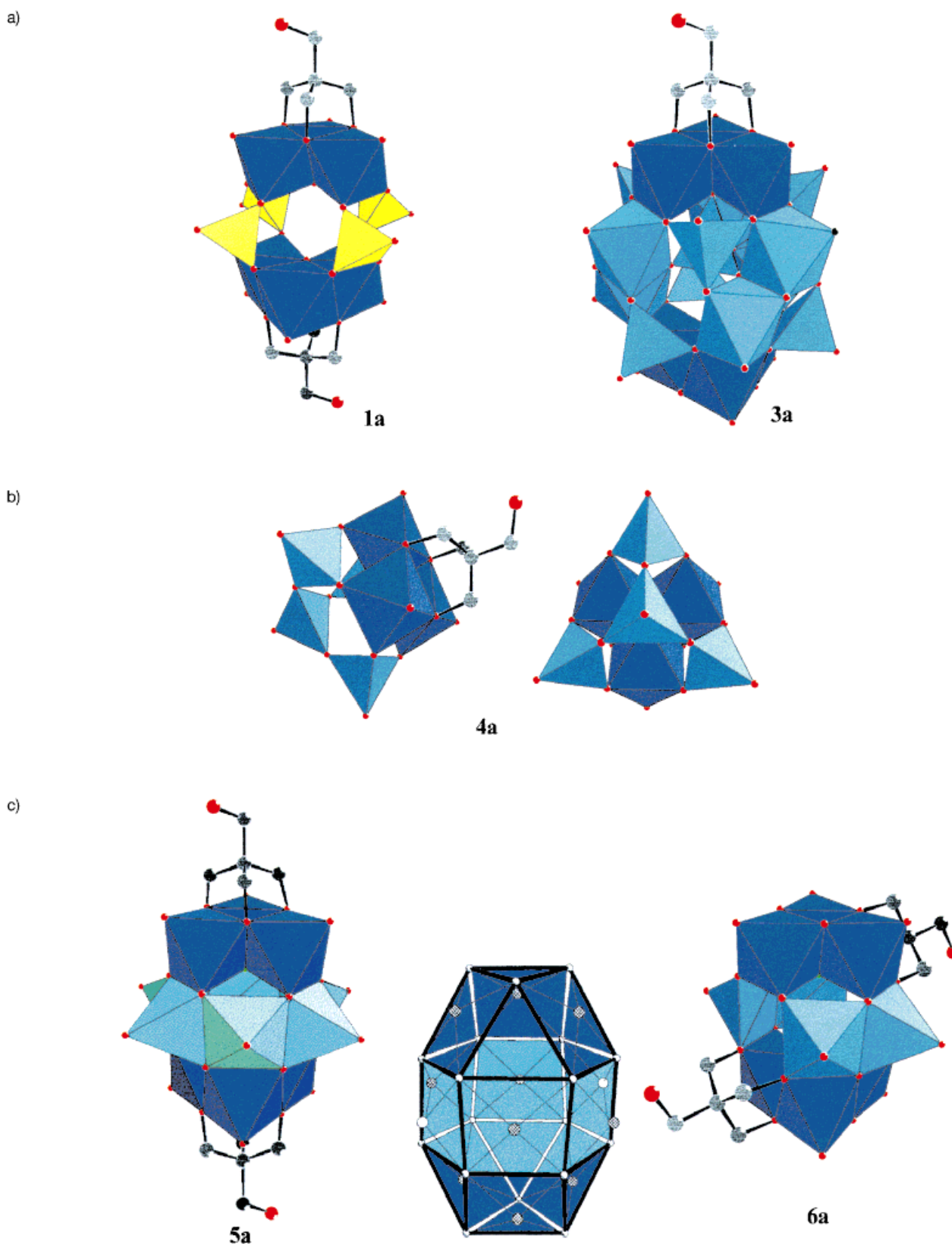


Figure 2. Polyhedral representation with ball-and-stick ligands of a) the anions **1a** and **3a**; b) two different views of **4a**; c) **5a** (proposed structure) and **6a**. Trinuclear $[V_3O_{13}]$ (**1a**, **3a**) and $[V_3O_{12}F]$ (**4a**–**6a**) fragment(s) are dark blue; $\{PO_4\}$ tetrahedra are yellow; different types of $\{VO_n\}$ polyhedra of the (complementary) cluster fragments are light blue. Additionally in c) (center), the solid (elongated triangular gyrobicupola^[10]) spanned by the 18 bridging oxygen atoms of the cluster anions **5a** and **6a** is shown, in which the crosshatched (**5a** and **6a**) and white spheres (**5a**) symbolize the $\{VO\}$ caps. In **1a** and **4a** the trinuclear units are quasi-isolated (see text).

Table 1. Data collection, intensity measurements and refinement parameters for **1–4** and **6**.

Compound	1	2	3	4	6
space group	$P\bar{1}$	$C2/c$	$P2_12_12_1$	$C2$	$P2_1/n$
a [pm]	1091.7(4)	2690.7(13)	1325.6(3)	1779.3(4)	1198.8(2)
b [pm]	1232.9(5)	1116.7(6)	1368.8(3)	1146.3(2)	1621.2(5)
c [pm]	1251.2(5)	1703.9(5)	3697.5(7)	1906.2(4)	1236.9(2)
α [°]	65.95(3)	90	90	90	90
β [°]	84.57(3)	98.38(3)	90	102.88(3)	102.45(1)
γ [°]	65.42(3)	90	90	90	90
V [10^6 pm ³]	1393(1)	5065(4)	6709(2)	3790(1)	2347(1)
Z	1	4	4	4	2
ρ_{calcd} [g cm ⁻³]	1.93	2.03	2.17	1.93	2.09
μ (Mo $K\alpha$; $\lambda = 71.073$ pm) [mm ⁻¹]	1.22	1.37	2.63	1.76	2.01
scan range (2θ) [°]	4–50	5–54	4–52	4–50	4–50
scan speed [° min ⁻¹] [a]	3.9–29.3	3.9–29.3	3.90–29.3	3.9–29.3	3.9–29.3
temperature [K]	193	294	294	188	193
no. of meas. refls. [b]	5393	5836	7549	3900	4474
no. of indep. refls.	4926	5530	7318	3546	4124
no. of unique obs. refls.					
($F > 4\sigma(F)$)	4131	4699	5426	2812	3086
no. of variables	360	343	764	466	326
$R = \sum F_o - F_c / \sum F_o $ [c]	0.067	0.054	0.079	0.083	0.046

[a] Scan mode: ω scan. [b] Check reflections measured every 97 reflections. [c] Flack parameters $-0.02(7)$ (**3**) and $-0.03(8)$ (**4**).

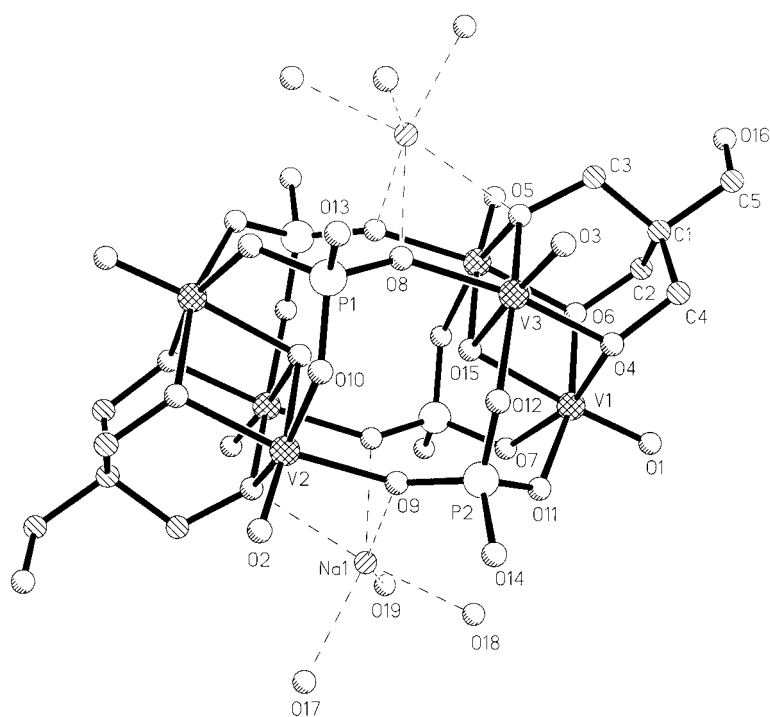


Figure 3. Ball-and-stick representation of the centrosymmetric anion of **1** including the Na⁺ ions and the oxygen atoms of the crystal water molecules coordinated with the latter.

ellipsoidal cluster and twisted with respect to each other by 60° (Figures 2, 5). The trinuclear units are linked by the other six {V^{IV}O₆} octahedra as well as six {V^VO₄} tetrahedra. The centre of the cluster is occupied by a tetrahedrally coordinated V^V atom, which is disordered over two positions in a 1:1 ratio in the crystal. Whereas in the case of **7** the six μ_2 -O atoms of the two trinuclear units are protonated, this is only true for one of the trinuclear units in **3** as the other unit is alkylated by the organic {(CH₂)₃CCH₂OH}³⁺ residue. Further protons are located at all the μ_2 -O positions, where two V^{IV} centres are

bridged (O34, O37, O39; Figure 5), and at the μ_3 -O atom of the trinuclear unit that is not linked to the central vanadium atom (O24 or O44, respectively, depending on the disorder). Bond valence sum calculations reveal that all vanadium atoms with octahedral coordination (mean valence sum: 4.05) are of the V^{IV} type and those with tetrahedral coordination are, as expected, of the V^V type (mean valence sum: 4.95, not considering the central, disordered vanadium atom V19/V19a for which the bond valence sum cannot be determined precisely). A remarkable structural feature of the anions of **3** and **7** is the presence of six V^{IV}–V^{IV} pairs with short V–V distances (mean value: 296 pm).

In the novel, aesthetically pleasing structure of the anion [{V₃L}V^V₄O₇]⁴⁻ (**4a**) of the mixed-valence compound **4** (space group $C2$), the μ_3 -O atom of the trinuclear unit in **1–3** is substituted by a μ_3 -F atom. The resulting {V₃O₁₂F} (\equiv {V₃L}') fragment is linked by six corners to three {V^VO₄} tetrahedra (Figures 2, 6) which are further connected through corners to a fourth {V^VO₄} tetrahedron in such a way that the entire anion adopts approximately C_{3v} symmetry when the terminal {CH₂OH} groups of the ligand are neglected. In contrast to the situation in the anion **1a**, the V–V distances within the trinuclear unit (with V^{IV} centres) are nearly identical (approximately 333 pm).

In the case of **5**, a single-crystal X-ray structure analysis could not be performed because of the insufficient quality of the crystals. However, comparison of the analytical, the spectroscopic and especially the magnetochemical data with those of the structurally closely related compound Na₆[H₆V₁₀V^V₂O₃₀F₂]·22H₂O (**8**),^[8,9] obtained under nearly identical experimental conditions in the absence of pentaerythritol, unambiguously proved the proposed structure of the anion **5a** (Figure 2), in which two {V₃L}' units are situated

Table 2. Characteristic physical data for compounds 1–6.

Compound	1	2	3	4	5	6
Colour	green	blue	black	black	black	black
IR $\bar{\nu}$ [cm ⁻¹]						
ν_{as} (CH ₂)	2920 (w) 2850 (w)	2920 (w) 2860 (w)	2860 (w)	2920 (w) 2860 (w)	2920 (w) 2860 (w)	2925 (w) 2850 (w)
δ (H ₂ O)	1660 (s)	1645 (s)	1625 (m)	1660 (vs)	1630 (s)	1655 (vs)
δ (CH ₂)	1465 (w) 1440 (w) 1405 (w)	1470 (w) 1450 (w) 1405 (w)		1465 (w) 1445 (w) 1410 (w)	1470 (w) 1445 (w) 1405 (w)	1475 (w) 1445 (w) 1390 (w)
ν_{as} (PO ₄)	1250 (w)	1250 (br, w)				
ν (C–O)	1095 (sh) 1070 (s) 1020 (vs)	1110 (s) 1070 (s) 1025 (s)	1120 (m) 1060 (w) 1025 (w)	1120 (m) 1065 (w) 1030 (w)	1120 (m) 1065 (w) 1030 (w)	1115 (m) 1065 (m) 1035 (w)
ν (V=O)	925 (vs)	960 (vs)	970 (vs)	960 (s) 930 (m)	960 (vs)	965 (vs)
ν_{as} { μ_n -O–V _n } (n = 2–4)	$\left\{ \begin{array}{l} 840 \text{ (m)} \\ 735 \text{ (m)} \\ 650 \text{ (m)} \\ 515 \text{ (m-s)} \\ 470 \text{ (m)} \end{array} \right.$	855 (m–s) 735 (m) 655 (w) 525 (s) 480 (s)	860 (m) 845 (m) 825 (vs) 725 (vs) 525 (s)	825 (vs) 710 (m) 535 (m)	645 (sh) 620 (s) 490 (s)	760 (s) 610 (s) 530 (m)
ν_{as} {P– μ_2 -O–V}						
ν_{as} {V– μ_2 -OH–V}						
ν_{as} {V– μ_2 -OR–V}						
UV/Vis/NIR ^[a]						
λ_{max} [nm]						
$\pi(\text{O}) \rightarrow \text{d}(\text{V})$	270	270	310	310	350	310
d → d	640, 900	650, 900	410	≈ 550 (br)	560, 800	≈ 700 (br)
IVCT			≈ 1300 (br)		≈ 1050 (br)	≈ 1150 (br)
ESR (4 K)						
g_{\parallel}/g_{\perp}	1.84/1.98					
A_{\parallel}/A_{\perp} [G]	182/65					
Characteristic bond valence sums						
V ^{IV}	3.92–4.16	3.99–4.05	3.98–4.15	3.93–4.18		4.41
V ^V			4.81–5.04 ^[b]	4.97–5.23		4.86–4.98
μ -OH	1.02–1.36	0.98–1.35	1.01–1.07 ^[b]			

[a] Solid-state spectra (see Experimental Section). [b] Exception: disordered, central V^V atom (V19 and V19a) and disordered μ_3 -OH group (O24 and O44) of the trinuclear units (see text).

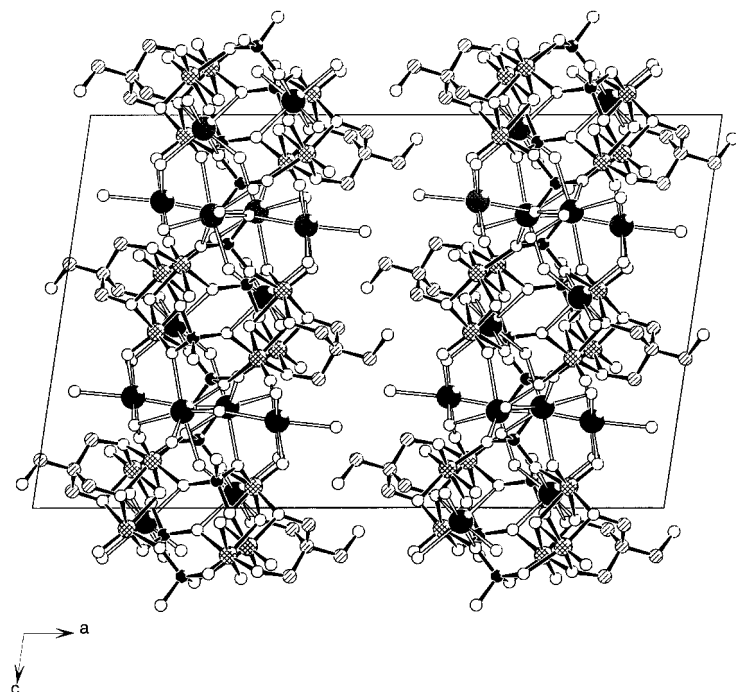


Figure 4. Representation of the stacking along the crystallographic *c* axis of the cluster anions of **2** (V: crosshatched; C: hatched; O: white spheres; P: small dark spheres) which are linked by the Na⁺ ions (largest spheres). The oxygen atoms of the crystal water molecules completing the coordination sphere of the Na⁺ cations are also shown.

above and below an equatorial belt built from six {VO₅} square pyramids (four {V^{IV}O₅} and two {V^VO₅}) and twisted with respect to each other by 60°. Formally, **5a** can be derived from the anion of **8** by replacing the six protons on the μ_2 -O atoms of the two trinuclear units by two {(CH₂)₃CCH₂OH}³⁺ moieties. The similarities in the temperature-dependent magnetic behaviour of **5** and **8**^[9] prove that the distribution of the V^{IV} and V^V centres within the cluster structure is identical. Bond valence sum calculations for **8** show that the two V^V centres are situated at two opposite positions of the equatorial ring of the six {VO₅} square pyramids.

A common structural feature of all the anions mentioned so far is the coordination of the ligands to all three V^{IV} centres of the trinuclear units. If the charge density of the latter is reduced as a result of partial oxidation (V^{IV} → V^V), other coordination patterns may occur. An example is the structure of the anion [(V₃L)²⁺V₄O₄]⁴⁻ (**6a**) of the mixed-valence compound **6**; this anion is built from two {V^{IV}V^VO₁₂F-(CH₂)₃CCH₂OH} (that is, {V₃L}'') fragments twisted with respect to each other by 60° and linked by four equatorial {V^VO₅} pyramids (Figures 2, 7). In the present case, the tripod ligand connects two vanadium centres (V2, V3') of the trinuclear unit with vanadium atoms of the equatorial belt. Bond valence sum

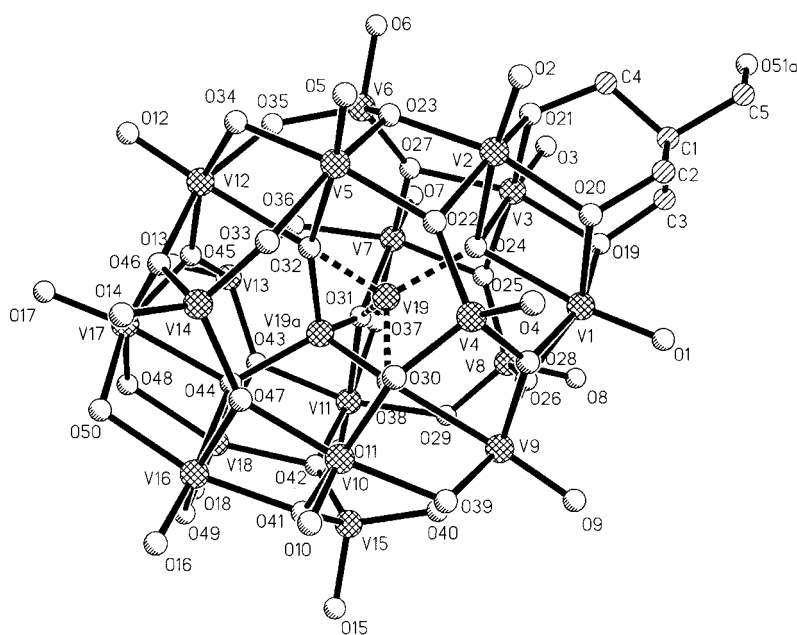


Figure 5. Ball-and-stick representation of the anion **3a** (disordered atoms marked "a").

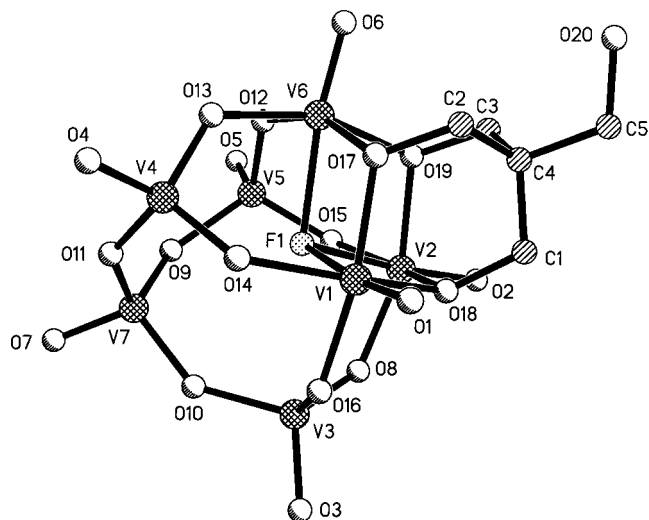


Figure 6. Ball-and-stick representation of the anion **4a**.

calculations are consistent with the oxidation state +IV for V5 and V5' atoms.

The anions **5a** and **6a** can be related topologically to each other by an interesting solid (an elongated triangular gyrobicupola), spanned by the 18 bridging oxygen atoms of the clusters, which has 12 square and six triangular planes corresponding to a hexagonal prism capped by two triangular cupolae twisted with respect to each other by 60° (Figure 2; see also ref. [10]). The structure of **5a** can be derived from this solid by capping all 12 square planes by {VO} groups and the two (001) triangular planes by the $\{(\text{CH}_2)_3\text{CCH}_2\text{OH}\}$ ligands. In **6a** two opposite square faces remain uncapped, whereas the organic ligands cap two of the six symmetry-equivalent triangular faces.

The IR spectra (see Table 2) are dominated by features attributed to vibrations of the V–O framework. The incor-

poration of the organic component is confirmed by bands assigned to $\nu_{\text{as}}(\text{CH}_2)$ (around 2900 cm^{-1}), $\delta(\text{CH}_2)$ (around 1450 cm^{-1}) and (less characteristic) $\nu(\text{C}-\text{O})$ vibrations (at approximately 1120 , 1070 and 1030 cm^{-1}). The alkylation of the trinuclear $\{\text{V}_3^{\text{IV}}\text{O}_{12}\text{F}\}$ units in the case of **5** is apparent when the spectra of the latter are compared with those of the non-alkylated compound **8**: the exchange $\mu_2\text{-OH} \rightarrow \mu_2\text{-OR}$ leads to the shift of a band (attributed to a vibration mainly localized in the $\{\text{V}-\mu_2\text{-O}(\text{H,R})-\text{V}\}$ fragment) from 670 cm^{-1} in the spectrum of **8** to 645 cm^{-1} in the spectrum of **5**. The influence of the cations on the vibrational frequencies of the cluster anion is apparent by comparison of the spectra of **1** and **2**, as the most intense $\nu(\text{V}=\text{O})$ -type band at 960 cm^{-1} in the spectrum of **2** is shifted to 925 cm^{-1} in the spectrum of **1**. The lower frequency in the case of **1** can be attributed to hydrogen bonds between the guanidinium cations and the terminal oxygen atoms of the $\{\text{V}=\text{O}\}$ groups.

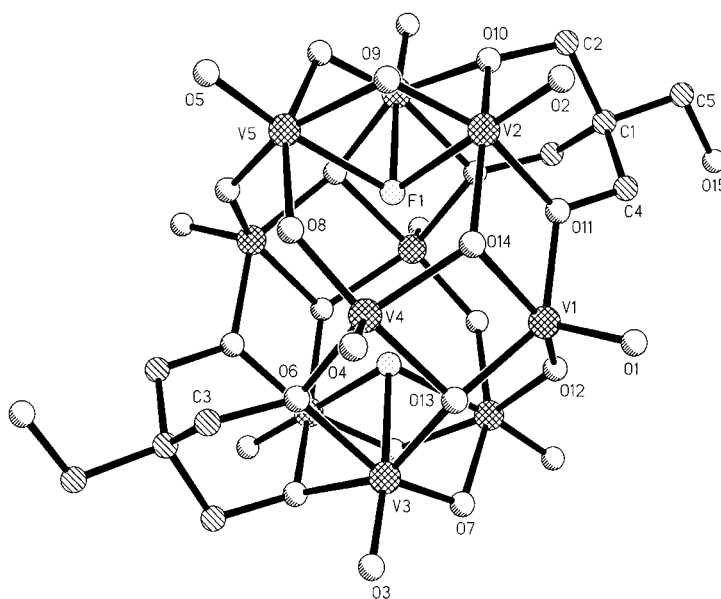


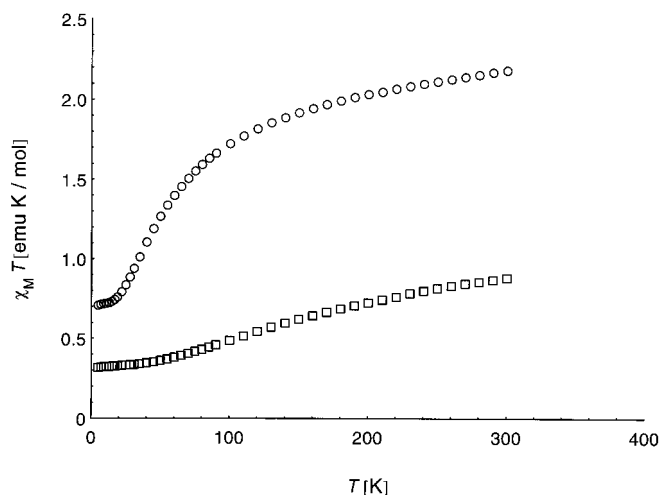
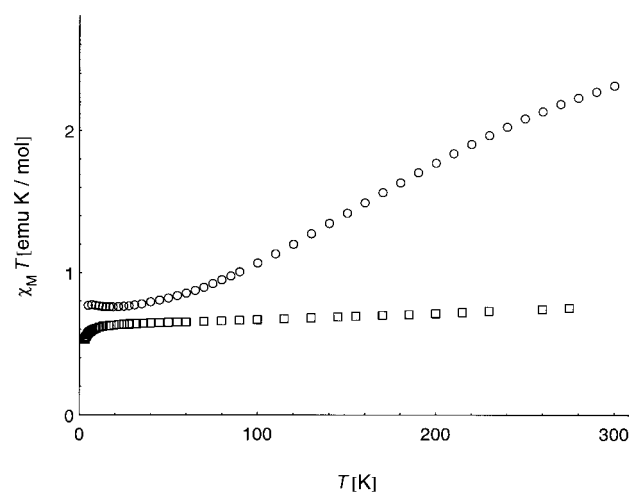
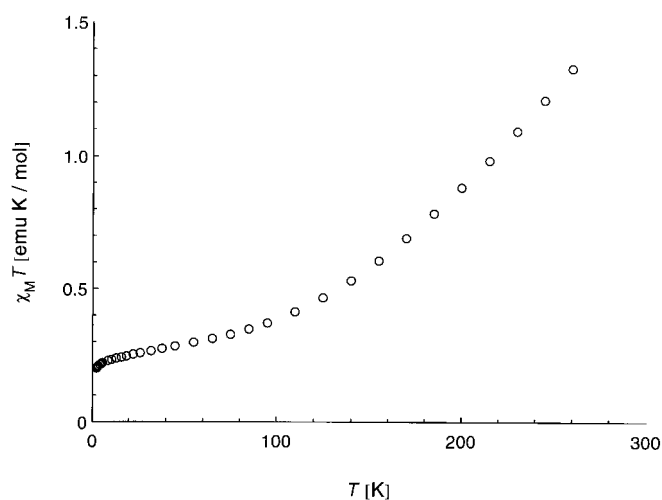
Figure 7. Ball-and-stick representation of the anion **6a**.

The bands in the electronic spectra can be assigned to charge-transfer (CT) transitions of the type $\pi(\text{O}) \rightarrow \text{d}(\text{V})$ (between 250 and approximately 400 nm), $\text{d} \rightarrow \text{d}$ and (high-energy) intervalence charge transfer (IVCT) transitions (between 400 and 950 nm) and low-energy IVCT transitions above 950 nm (Table 2).

The investigation of the interaction between the V^{IV} centres by measuring the magnetochemical properties is especially interesting (Table 3) and makes it possible to determine whether the trinuclear units are electronically isolated. Figures 8–10 show the temperature dependence of the measured susceptibilities of the compounds **1**, **3** and **4–6**. In all cases antiferromagnetic coupling occurs, but there are

Table 3. Magnetochemistry as an analytical tool for the characterization of polyvanadates with trinuclear $\{V_3O_{13}\}$ or $\{V_3O_{12}F\}$ units, respectively.

Compound	1	3	4	5	6
Number and type of trinuclear units	2 $\{V_3^{IV}\}$	2 $\{V_3^{IV}\}$	1 $\{V_3^{IV}\}$	2 $\{V_3^{IV}\}$	2 $\{V^{IV}V_2^V\}$
$\chi_M T$ (260 K) [emu K mol^{-1}]	2.12	1.34	0.83	2.13	0.74
$\chi_M T$ (260 K)/ V^{IV} [emu K mol^{-1}]	0.35 (\approx spin-only value)	0.11 (strong antiferromagnetic interaction)	0.27 (weak antiferromagnetic interaction)	0.21 (strong antiferromagnetic interaction)	0.37 (spin-only value)
magnetic interaction of the V^{IV} centre(s) of the trinuclear unit with other centres	very weak	very strong	quasi-isolated $\{V_3\}'$ unit	strong	negligible
plateau at $T < 20$ K $\chi_M T$ [emu K mol^{-1}]	≈ 0.72		≈ 0.33	≈ 0.75	
uncorrelated spins ($T < 20$ K)	2		1	2	

Figure 8. Temperature dependence of $\chi_M T$ for **1** (○) and **4** (□).Figure 10. Temperature dependence of $\chi_M T$ for **5** (○) and **6** (□).Figure 9. Temperature dependence of $\chi_M T$ for **3** (○).

characteristic differences. Whereas the $\chi_M T$ value at 300 K (2.18 emu K mol^{-1}) for **1** is approximately identical to the spin-only value for six independent V^{IV} (d^1) centres (2.23 emu K mol^{-1}), reduction of the temperature leads to a decrease in $\chi_M T$, which reaches a plateau below 20 K (Figure 8). [In the high-temperature region, **1** exhibits approximately Curie–Weiss behaviour ($\Theta = -49$ K)]. The value corresponding to the plateau (0.72 emu K mol^{-1}) is a clear indication of the presence of two electrons with essentially

uncorrelated spins. The corresponding spin ground state for each of the two individual triangles, composed of three interacting spins, is expected to be a degenerate $S = 1/2$ state. The results of an EPR-spectroscopic investigation shown in Figure 11 confirm this expectation. Whereas above 40 K only one broad signal at $g \approx 1.90$ can be detected, a hyperfine splitting of this signal into eight lines occurs when the temperature is lowered. The spectrum at 4 K is typical of an uncorrelated spin, being located mainly at one ^{51}V ($I = 7/2$) centre. A simulation of the spectrum gives $g_{\parallel} = 1.84$, $g_{\perp} = 1.98$, $A_{\parallel} = 182$ G, $A_{\perp} = 65$ G.

Comparable magnetic behaviour is observed in the case of **4**. The graph of $\chi_M T$ versus T has a plateau at 0.33 emu K mol^{-1} below approximately 40 K, indicating the presence of one electron with an uncorrelated spin within the triangle spanned by the V^{IV} centres (Figure 8). The high-temperature data (100 K $< T < 300$ K) indicate Curie–Weiss behaviour ($\Theta = -215$ K).

The $\chi_M T$ value at 260 K (1.34 emu K mol^{-1} ; Figure 9) of **3** is much lower than the spin-only value for the 12 V^{IV} centres (4.46 emu K mol^{-1}). This observation has to be attributed to a very strong antiferromagnetic interaction within the six V^{IV} – V^{IV} pairs in the cluster with a mean distance of 296 pm (see the structural data above). The strong antiferromagnetism is also apparent from the fact that $\chi_M T$ decreases dramatically with decreasing temperature in the region 100 K $< T < 260$ K (for a discussion, see ref. [11]).

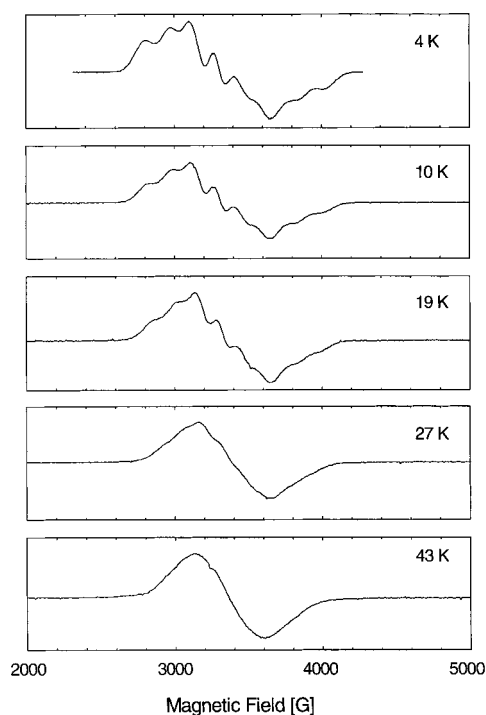


Figure 11. EPR spectrum of **1** at various temperatures.

Similarly, the room-temperature $\chi_M T$ value of $2.3 \text{ emu K mol}^{-1}$ measured for **5** is much lower than expected for ten uncorrelated spins ($3.75 \text{ emu K mol}^{-1}$), again indicating the presence of strong antiferromagnetic interactions within the cluster. This is confirmed by the monotonic reduction in $\chi_M T$ with decreasing temperature down to a plateau at a $\chi_M T$ value of $0.75 \text{ emu K mol}^{-1}$ below 50 K (Figure 10), which is a clear indication of the presence of two electrons with essentially uncorrelated spins. As nearly the same magnetic behaviour is observed for the non-alkylated compound **8**, the structure of which is known,^[9] both anions must be assumed to have a practically identical structure with an identical spatial distribution of the paramagnetic centres. This conclusion is important as it was not possible to apply single-crystal X-ray structure analysis to **5** because of the poor quality of the crystals. A detailed description and interpretation of the magnetic behaviour of **8** is given in reference [9].

The high-temperature $\chi_M T$ value of $0.75 \text{ emu K mol}^{-1}$ obtained for **6** confirms the presence of two V^{IV} centres, which is also consistent with the results of bond valence sum calculations and redox titrations (Figure 10). Compound **6** exhibits Curie–Weiss behaviour with a low value of the Weiss constant ($\theta = -3 \text{ K}$), which indicates that the magnetic exchange interactions between the two 3d electrons are only small. The results of the magnetochemical studies are summarized in Table 3.

Conclusion




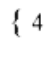
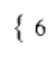
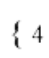


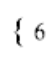
The elucidation of the basic principles responsible for the formation of the overwhelming variety of complex polyoxo-

ometallate clusters is a challenge. Unfortunately, however, the possibilities of investigating the related, rather complex, reactions in solution are limited. Therefore, the only practicable—although not unproblematic—method is to determine a large number of the crystal structures of the precipitates and to try to draw conclusions about possible situations in solution.

Since trinuclear units of the type $\{\text{M}_3\text{O}_{13}\}$ are abundant as fragments in polyoxometallate structures it can be assumed that these units can be generated in solution—at least when they are attached to other fragments—during the primary processes of structure formation. In the special case of polyoxovanadate systems ($\text{M} = \text{V}$), the high charge density of these units leads to a strong tendency towards the formation of highly condensed clusters with the $\{\text{V}_{12}\text{O}_{36}(\text{VO})_6\}$ shell.^[12] However, the presence of an organic ligand with appropriate geometry favours the formation of the trinuclear units, which are stabilized as fragments through a partial reduction of the charge and shielded to some extent from further capping with electrophilic $\{\text{VO}\}^{n+}$ units. In this way cluster anions such as **1a**, **2a** or **4a** can be obtained, in which the trinuclear units are present in a quasi-isolated form sharing only corners (in contrast to **3a**, for example) with other polyhedra. In the absence of the organic ligand, structures of this kind have not been observed. The high charge density of the trinuclear fragments can also be reduced by multiple protonation. However, units of the latter type are known so far only as integral parts of larger cluster aggregates (as in the anions of **7** and **8**). The data in Table 4 illustrate formally the nucleation process directed by the trinuclear fragments.

Under the conditions used for the syntheses of the clusters described here (in aqueous media with various pH values, in the presence of a tripod ligand, at moderate reaction temperatures, at normal pressure) trinuclear units have—in the sense mentioned above—a high tendency to form and to induce or influence, as nucleation cores, the aggregation of the other building units by an (induced) self-assembly process. The understanding of the charge control of the structure-forming processes is of great significance, as mentioned in the Introduction. The charge on the trinuclear units can vary to a small extent because of changes in protonation, alkylation, the number of reduced metal centres and the substitution of O^{2-} by F^- . Interestingly, the sum of the charges on the other building units completing each of the cluster structures also has a relatively constant value corresponding to the related (charge) complementary fragments (Table 4). Comparison of the structurally related anions of **5** and **6** makes it apparent that a higher negative charge on the trinuclear units favours a higher nuclearity of the cluster. Another successful way to increase the cluster size could be based on the possibility of increasing the number of incorporated trinuclear units that are stabilized by an organic ligand (consider, in this context, the synthesis of $(\text{Me}_3\text{NH})_2(\text{Et}_4\text{N})\text{Na}_4[\text{Na}(\text{H}_2\text{O})_3\text{H}_{15}\text{Mo}_{42}\text{O}_{109}\{(\text{OCH}_2)_3\text{CCH}_2\text{OH}\}_7] \cdot 15 \text{H}_2\text{O}$ ^[13]). In general, the variety of aggregation patterns in the chemistry of polyoxovanadates with vanadium in the oxidation states +IV and +V seems to be much more diverse than in the case of polyoxomolybdates or polyoxotungstates.

Table 4. Trinuclear fragments and complementary fragments defined formally by their mononuclear building units {.....}^{n±} corresponding to Figure 2 with formal charge values in the second and third columns.

Species	Type (and number) of trinuclear fragment ^[a]	Complementary fragments {.....} ^{n±} as defined by their mononuclear building units ^[a]	Polyhedral representation of the mononuclear building units according to column 3 ^[c]	Total charge
1a	{HV ^{IV} O ₇ L(OH) ₆ } ⁴⁻ (2) ^[b]	{2H; {4OP(OH) ₃ } ²⁺ }	{ 4  }	6-
3a	{HV ^{IV} O ₇ L(OH) ₆ } ⁴⁻ (1) + {H ₃ V ^{IV} O ₆ (OH) ₇ } ⁴⁻ (1) ^[d]	{3H; 3{OV ^{IV} (OH) ₂ (OH ₂) ₃ }; 3{OV ^{IV} (OH) ₃ (H ₂ O) ₂ }; 6{OV ^V (OH) ₃ }; {V ^V (OH) ₄ } ⁺ }	{ 6  7  }	7-
4a	{V ^{IV} O ₆ F L(OH) ₆ } ⁴⁻ (1)	{4{OV ^V (OH) ₃ } ⁰ }	{ 4  }	4-
5a	{V ^{IV} O ₆ F L(OH) ₆ } ⁴⁻ (2)	{4{OV ^{IV} (OH) ₂ (OH ₂) ₂ }; 2{OV ^V (OH) ₂ (OH ₂) ₂ } ²⁺ }	{ 6  }	6-
6a	{V ^{IV} V ^V O ₆ F L(OH) ₆ } ²⁻ (2)	{4{OV ^V (OH) ₃ (OH ₂) ₂ } ⁰ }	{ 4  }	4-
7a ^[7]	{H ₄ V ^{IV} O ₇ (OH) ₆ } ⁴⁻ (1) + {H ₃ V ^{IV} O ₆ (OH) ₇ } ⁴⁻ (1)	{3H; 3{OV ^{IV} (OH) ₂ (OH ₂) ₃ }; 3{OV ^{IV} (OH) ₃ (H ₂ O) ₂ }; 6{OV ^V (OH) ₃ }; {V ^V (OH) ₄ } ⁺ }	{ 6  7  }	7-
8a ^[8]	{H ₃ V ^{IV} O ₆ F (OH) ₆ } ⁴⁻ (2)	{4{OV ^{IV} (OH) ₂ (OH ₂) ₂ }; 2{OV ^V (OH) ₂ (OH ₂) ₂ } ²⁺ }	{ 6  }	6-

[a] The groups which are involved in the (formal) linking of structural elements are written in *italics*. The corresponding protons of the OH groups are no longer present in the final cluster structure because the related condensation process occurs with concomitant loss of H₂O. The H₂O groups act as leaving groups for μ₃-O connections and therefore do not appear in the balance (final formula). Protons occurring in the final structure are written at the beginning of the bracket. [b] L = (CH₂)₃CCH₂OH. [c] These occur in the final structure ({PO₄} as a tetrahedron (yellow); {VO_x} as tetrahedra, octahedra and square pyramids (light blue)). [d] Formulated for one of the disordered positions of the central V atom.

Experimental Section

Materials: All reagents were obtained from normal commercial sources and used without further purification. NaVO₃ was prepared from NaOH and V₂O₅.

Preparation of (CN₃H₆)₄Na₂[H₄V^{IV}P₄O₃₀{(CH₂)₃CCH₂OH}₂]·14H₂O (1): To a solution of VOSO₄·5H₂O (3.2 g, 12.6 mmol) in a mixture of 85% H₃PO₄ (3 mL, 44 mmol) and distilled water (50 mL), pentaerythritol (3.4 g, 25.0 mmol) and guanidine hydrochloride (CN₃H₆Cl) (1.2 g, 12.5 mmol) were added and the solution was kept for 30 min at 70–75 °C in a 100-mL Erlenmeyer flask covered with a watch glass. The pH was subsequently adjusted to approximately 8 with 10M NaOH solution. During the addition of NaOH a grey precipitate was formed which redissolved at higher pH values. After the reaction mixture had been kept for a further 5 h at 70–75 °C, the green solution was filtered and the filtrate was allowed to stand at 20 °C for three days. The precipitated green crystals of **1** were filtered off, washed with cold water and dried on filter paper. Yield 2.8 g (82% based on V); C₁₄H₇₄N₁₂Na₂P₄O₄₆V₆ (1621.5): calcd C 10.36, H 4.56, N 10.36, Na 2.8; found C 10.41, H 4.58, N 10.15, Na 3.2.

Preparation of Na₆[H₄V^{IV}P₄O₃₀{(CH₂)₃CCH₂OH}₂]·18H₂O (2): The method of synthesis was analogous to that of **1** but without the addition of guanidine hydrochloride. The blue crystals, which precipitated after three days, were washed with cold water and dried on filter paper. Yield 2.7 g (83% based on V); C₁₀H₅₈Na₆P₄O₅₀V₆ (1545.5): calcd C 7.76, H 3.75, Na 8.9; found C 7.73, H 3.76, Na 9.0.

Preparation of (NH₄)₇[H₇V^{IV}V^VO₃₀{(CH₂)₃CCH₂OH}]·11.5H₂O (3): A solution of NH₄VO₃ (8.0 g, 68.4 mmol) in H₂O (250 mL) was treated at 80 °C with hydrazine sulfate (N₂H₆SO₄) (1.37 g, 10.5 mmol) and pentaerythritol (2.93 g, 21.5 mmol) in a 300-mL narrow-necked Erlenmeyer flask covered with a watch glass. The resulting dark brown solution was stirred for 10 min at 80 °C; the pH was subsequently adjusted with H₂SO₄ (10%) to 5.3–5.4. After 5 h the hot solution was filtered and the filtrate was allowed to stand for three days to crystallize at 20 °C. The precipitated black,

octahedral crystals of **3** were isolated, dried on filter paper and stored under argon. Yield 3.4 g (43% based on V); C₅H₆₇N₇O_{62.5}V₁₉ (2192.9): calcd C 2.74, H 3.06, N 4.47; found C 2.64, H 3.31, N 4.21.

Preparation of (CN₃H₆)₄[V^{IV}V^VO₁₉F(CH₂)₃CCH₂OH]·5.25H₂O (4): A solution of NaVO₃ (3.05 g, 25 mmol) in H₂O (25 mL) was treated with hydrazine hydrate (182 μL, 100%, 3.75 mmol) at 80 °C and the resulting dark brown solution was kept for 1 h at that temperature without stirring in a 50-mL wide-necked Erlenmeyer flask covered with a watch glass. Pentaerythritol (1.14 g, 8.4 mmol), guanidine hydrochloride (2.0 g, 20.9 mmol) and HF (660 μL, 38–40%) were then added. After the solution had been allowed to stand on a heating plate at 80 °C for 2.5 h without being stirred, it was cooled to 40 °C and a blackish-grey precipitate was filtered off; the filtrate was kept at room temperature for one day. The precipitate of black needle-shaped crystals of **4** was isolated, dried on filter paper and stored under argon. Yield 1.1 g (28% based on V); C₉H_{43.5}FN₁₂O_{25.25}V₇ (1099.1): calcd C 9.83, H 3.96, F 1.7, N 15.26; found C 10.22, H 3.97, F 2.4, N 15.05.

Preparation of Na₆[V^{IV}V^VO₃₀F₂{(CH₂)₃CCH₂OH}₂]·22H₂O (5): A solution of NaVO₃ (3.05 g, 25 mmol) in H₂O (25 mL) was treated with hydrazine hydrate (182 μL) (100%, 3.75 mmol) at 90 °C and kept in a 50-mL wide-necked Erlenmeyer flask covered with a watch glass for 1 h at this temperature without being stirred. Pentaerythritol (1.71 g, 12.6 mmol) was added, then the pH was adjusted to 7 with HF (38–40%) and kept constant for the next 30 min by further addition of HF at intervals of approximately 3 min. The solution was allowed to stand at 90 °C for a further 1.5 h (during which the pH value did not exceed 7.0), then filtered; the filtrate was kept at 90 °C again for 3 h before it was cooled to about 20 °C. After one day the solution was filtered again to remove small amounts of a by-product. Small black crystals of **5** were isolated after two further days, dried on filter paper and stored under argon. Yield 0.5 g (13% based on V); C₁₀H₆₂F₂Na₆O₅₄V₁₂ (1833.3): calcd C 6.55, H 3.38, F 2.1, Na 7.5, H₂O 21.6; found C 6.70, H 3.83, F 2.2, Na 7.5, H₂O 22.0.

Preparation of (CN₃H₆)₄[V^{IV}V^VO₂₈F₂{(CH₂)₃CCH₂OH}₂]·4H₂O (6): Compound **4** (0.8 g, 0.7 mmol) was dissolved in distilled water (20 mL) at

80 °C in a 50 mL wide-necked Erlenmeyer flask covered with a watch glass and the pH of the solution was adjusted with HF (38–40%) to about 3.5. After addition of H₂O₂ (125 µL, approximately 30%) the reaction mixture was kept at 80 °C for 30 min, cooled to room temperature and filtered. From the filtrate black crystals of **6** were isolated after 2–3 days and dried on filter paper. Yield 0.1 g (17% based on V); C₁₄H₅₀F₂N₁₂O₃₄V₁₀ (1477.4); calcd C 11.37, H 3.38, F 2.6, N 11.37; found C 11.02, H 3.34, F 3.0, N 11.51.

Crystal structure analyses: The structures were determined from single-crystal X-ray diffraction data (Siemens R3m/V four-circle diffractometer). Crystal data and details concerning the intensity data collection and structure refinement are given in Table 1. Unit cell parameters were obtained by least-squares refinements of the angular settings of 15 high-angle reflections ($20^\circ < 2\theta < 30^\circ$). An empirical absorption correction was applied for all compounds and the data were corrected for Lorentz and polarization effects. Structures were solved by direct methods (SHELXTL program package).^[14] Final least-squares refinements converged at values given in Table 1. Atomic scattering factors for all atoms were taken from standard sources^[15] and anomalous dispersion corrections were applied to all atoms. Further details of the crystal structure investigations may be obtained from the Fachinformationszentrum Karlsruhe, 76344 Eggenstein–Leopoldshafen (Germany), on quoting the depository numbers CSD-408259 (**1**), 408260 (**2**), 408261 (**3**), 408262 (**4**), 408263 (**6**).

Spectroscopic and magnetochemical investigations and chemical analyses: Infrared spectra were measured on a Bruker IFS 66 FRA 106 instrument and the electronic spectra on a Beckman Acta MIV instrument (UV/Vis by solid-state reflectance by means of an Ulbricht sphere with cellulose as calibration standard; NIR with KBr pellets in transmission). For the magnetic susceptibility measurements, various SQUID magnetometers were used (Metronique Ingenierie, University of Florence; Quantum Design, Universität Bonn and Universität Bielefeld) with an applied field of 10 kOe. The EPR spectrum was recorded on a polycrystalline powder at X-band frequency on a Varian E-9 spectrometer. Variable temperatures were achieved with a liquid-helium continuous-flow cryostat. Whereas the C, H, N analyses were carried out in our laboratory using a Perkin-Elmer 420 element analyser, the F analyses were performed by the Microanalytical Laboratory Beller in Göttingen (Germany). The number of V^{IV} centres in the compounds was determined by potentiometric titration with 0.02 M KMnO₄ solution using a Mettler DL 40 memotitrator (Pt/calomel electrode). Crystal water was determined by TGA with a Linseis L81 instrument.

Acknowledgments: We thank Prof. Dr. D. Gatteschi, Dr. Roberta Sessoli and M. Ahle (University of Florence) as well as Prof. Dr. M. Jansen and N. Wagner (Universität Bonn) for the magnetic susceptibility measurements, and Dr. R. Sessoli additionally for help with the simulation of the EPR spectrum. We also thank the Deutsche Forschungsgemeinschaft and the Fonds der Chemischen Industrie for financial support.

Received: January 26, 1998 [F976]

- [1] a) M. T. Pope, A. Müller, *Angew. Chem.* **1991**, *103*, 56–70; *Angew. Chem. Int. Ed. Engl.* **1991**, *30*, 34–48; b) A. Müller, H. Reuter, S. Dillinger, *ibid.* **1995**, *107*, 2505–2539 and **1995**, *34*, 2328–2361; c) A. Müller, C. Beugholt, *Nature (London)* **1996**, *383*, 296–297.
- [2] M. T. Pope, *Heteropoly and Isopoly Oxometalates*, Springer, Berlin, **1983**.
- [3] a) R. Kato, A. Kobayashi, Y. Sasaki, *J. Am. Chem. Soc.* **1980**, *102*, 6571–6572; b) D. Hou, K. S. Hagen, C. L. Hill, *J. Chem. Soc. Chem. Commun.* **1993**, 426–428.
- [4] A. Müller, J. Döring, H. Bögge, E. Krickemeyer, *Chimia* **1988**, *42*, 300–301.
- [5] a) Q. Chen, D. Goshorn, C. Scholes, X. Tan, J. Zubieta, *J. Am. Chem. Soc.* **1992**, *114*, 4667–4681; b) M. I. Khan, Q. Chen, J. Zubieta, D. P. Goshorn, *Inorg. Chem.* **1992**, *31*, 1556–1558; c) M. I. Khan, Q. Chen, D. P. Goshorn, H. Hope, S. Parkin, J. Zubieta, *J. Am. Chem. Soc.* **1992**, *114*, 3341–3346; d) M. I. Khan, Q. Chen, H. Hope, S. Parkin, C. J. O'Connor, J. Zubieta, *Inorg. Chem.* **1993**, *32*, 2929–2937; e) M. I. Khan, Q. Chen, D. P. Goshorn, J. Zubieta, *ibid.* **1993**, *32*, 672–680; f) M. I. Khan, Y.-S. Lee, C. J. O'Connor, J. Zubieta, *J. Am. Chem. Soc.* **1994**, *116*, 5001–5002.
- [6] I. D. Brown in *Structure and Bonding in Crystals, Vol. II* (Eds.: M. O'Keeffe, A. Navrotsky), Academic Press, New York, **1981**, pp. 1–30.
- [7] A. Müller, M. Penk, E. Krickemeyer, H. Bögge, H.-J. Walberg, *Angew. Chem.* **1988**, *100*, 1787–1789; *Angew. Chem. Int. Ed. Engl.* **1988**, *27*, 1719–1721.
- [8] A. Müller, R. Rohlfing, E. Krickemeyer, H. Bögge, *Angew. Chem.* **1993**, *105*, 916–918; *Angew. Chem. Int. Ed. Engl.* **1993**, *32*, 909–912.
- [9] A. Müller, R. Rohlfing, A.-L. Barra, D. Gatteschi, *Adv. Mater.* **1993**, *5*, 915–917.
- [10] A. Müller, M. Penk, J. Döring, *Inorg. Chem.* **1991**, *30*, 4935–4939, and references therein.
- [11] A. Müller, R. Rohlfing, J. Döring, M. Penk, *Angew. Chem.* **1991**, *103*, 575–577; *Angew. Chem. Int. Ed. Engl.* **1991**, *30*, 588–590.
- [12] A. Müller, R. Sessoli, E. Krickemeyer, H. Bögge, J. Meyer, D. Gatteschi, L. Pardi, J. Westphal, K. Hovemeier, R. Rohlfing, J. Döring, F. Hellweg, C. Beugholt, M. Schmidtman, *Inorg. Chem.* **1997**, *36*, 5239–5250.
- [13] M. I. Khan, Q. Chen, J. Salta, C. J. O'Connor, J. Zubieta, *Inorg. Chem.* **1996**, *35*, 1880–1901.
- [14] G. M. Sheldrick, SHELXTL, Siemens Analytical X-Ray Instruments, Madison, WI (USA), **1994**.
- [15] *International Tables for Crystallography, Vol. C*, Kluwer, Dordrecht, **1992**.